Journal of the Chinese Chemical Society, 1990, *37*, 255-263

PREPARATION AND CATALYTIC PROPERTIES OF TRANSITION METAL DOPED ZSM-5 ZEOLITES

BEN-ZU WAN*(萬本儒) and TRAN CHIN YANG(楊燦欽)
Department of Chemical Engineering, National Taiwan University, Taipei, Taiwan, R.O.C.

Metal silicates of ZSM-5 type structure were prepared by doping silicate gels with chromium, manganese, cobalt, nickel, and copper ions, respectively, followed by reacting hydrothermally. The resultant materials were characterized by the metal content, x-ray powder diffraction, ion exchange capacity, surface area, thermal stability, and temperature programmed desorption of ammonia for acidity measurement. In addition, the catalytic properties of these metal silicates were examined using ethanol conversion as a probe reaction. The effect of transition metal content on the catalysis for dehydration, dehydrogenation, oligomerization, cracking, and cyclization to the aromatics was established and compared with that of HZSM-5 catalyst.

INTRODUCTION

The unique properties of ZSM-5 zeolite as a catalyst for reactions and as a molecular sieve for adsorption have been well documented[1-7]. Recently, there has been growing attention paid to the incorporation of metals other than aluminum within ZSM-5 during crystal growth, in order to obtain different acidity and catalytic activity within crystals[8-13]. Miyamoto *et al.*[8] and Inui *et al.*[13] described synthetic procedures of vanadosilicate. It was found that a resultant catalyst of high crystallinity was effective for methanol to hydrocarbon conversion, while that of low crystallinity was favorable for ammoxidation of xylene and reduction of nitrous oxide. Szostak *et al.*[9], Kotasthane *et al.*[10], Borade[11], and Inui *et al.*[12] performed the synthesis and characterization of crystalline ferrisilicate of ZSM-5 structure. The catalyst showed higher activity for the production of C_2-C_4 from methanol conversion[12], and lower activity for xylene isomerization than HZSM-5[11].

The present paper describes the preparation and characterization of catalytic properties of metal silicates with ZSM-5 structure. Incorporated metal ions were either chromium, manganese, cobalt, nickel, or copper ions. The catalytic activities of these catalysts were evaluated and compared with those of HZSM-5 via ethanol conversion.

EXPERIMENMTAL

Catalysts

Metal silicates of ZSM-5 structure were prepared by hydrothermal crystallization. Each metal silicate series was prepared with three to four different M/Si mole ratios. The mole ratios in the gel mixtures were SiO_2:M:TPABr:NaOH:H_2O = 0.78:x:0.03:0.2:10, where M = metal and x = 0.01, 0.005 or 0.0025. Silicalite was also prepared without addition of any metal ions. After stirring for half an hour, each gel mixture was heated in a polypropylene bottle at 373K for seven days. The resultant crystalline products were washed with deionized water, and dried at room temperature. Proton form samples were prepared by calcination of the washed products in air at 773K for six hours, exchanging three times with 0.5M ammonium sulfate solution at room temperature, then washing, drying, and calcination again.

Apparatus

The x-ray powder diffraction patterns were taken with a Phillips PW1729 with Cu$K\alpha$ radiation. The thermal stabilities were determined with a ULVAC TGD-7000RH thermal analyzer (TGA and DTA) from room temperature to 1273K. The BET surface area was measured on a

Micromeritic Accusorb 2100D unit. The elemental content of each sample was determined by an atomic absorption unit (model IL151 Instrumentation Laboratory Inc.). The acidic strength was measured by temperature programmed desorption (TPD) of ammonia, using a TCD detector and nitrogen (99.999%) carrier gas. Prior to the ammonia adsorption, samples were pre-heated to 823K under a 60 mL/min nitrogen flow. Ammonia adsorption was made at room temperature for thirty minutes. After purging away ammonia in the bulk of the reactor, the TPD of ammonia was carried out at temperature increasing rate of 10 K/min under a 60 mL/min nitrogen flow.

In the ethanol conversion reaction, 0.5g of catalyst was used at 623K and under atmospheric pressure. Pure liquid ethanol was fed into the reactor (3/8 inch, SS) by a Milton Roy mini pump with WHSV = 3.2 h^{-1}. Ethanol was vaporized at 373K prior to entering the reactor. The reaction temperature was monitored with a K type thermocouple within a thermowell inside the reactor. The downstream of the reactor maintained the temperature about 393K in order to prevent product condensation. The liquid products were collected in the condensor every hour. Both liquid and gas products were analyzed with a Shimadzu GC-8A gas chromatography. A Porapak S column was used for separation.

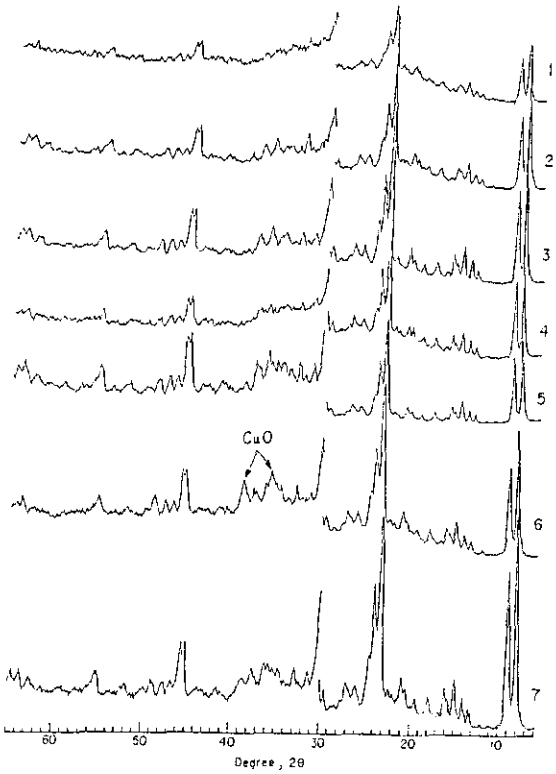

Fig. 1. XRD patterns of silicalite and metal silicate. Peak intensity is doubled for 2θ larger than 30. 1. calcined silicalite; 2. calcined chromium silicate; 3. calcined manganese silicate; 4. calcined cobalt silicate; 5. calcined nickel silicate; 6. calcined copper silicate; 7. ammonium exchanged copper silicate.

RESULTS AND DISCUSSION

X-ray Powder diffraction patterns

The ZSM-5 structure of the pentasil family was identified by the XRD pattern[14]. Figure 1 shows that the ZSM-5 structures were maintained after the synthesized samples were calcined at 773K under air for six hours. The calcined copper silicate contained a trace amount of cupric oxide, as shown in Figure 1.6 of XRD peaks at $2\theta = 36$ and 39 [15]. The intensity of CuO peaks decreased after the sample was converted to the proton form (Figure 1.7). Furthermore, the XRD patterns of the calcined samples showed that the crystallinities increased after the metal silicates were exchanged with ammonium sulfate solution. This suggests that the exchange procedure may remove some of amorphous material from the samples.

Molar ratios of metal to silicon and BET surface areas

The molar ratios of metal to silicon and BET surface areas of the synthesized metal silicates before and after the ammonium exchange are listed in Table 1. The results show that the metal to silicon ratios were higher in the solid product than in the gels. Similar phenomena were also observed in the synthesis of ZSM-5 in which aluminum was found easily to incorporate within the crystal structure[16].

Table 1. Metal to Silicon Ratio and BET Surface Area[a] of Metal Silicate with ZSM-5 Structure

transition metal in Silicate	M^b/Si, mole ratio in the gel	after crystallization	after ammonium treatment[c]	Al/Si mole ratio	BET surface area m^2/g
-	1.3×10^{-2}	3.6×10^{-2}	8.4×10^{-4}	2.7×10^{-3}	253
Cr	6.4×10^{-3}	2.3×10^{-2}	6.1×10^{-4}	--	296
-	3.2×10^{-3}	1.3×10^{-2}	4.1×10^{-5}	--	384
-	1.3×10^{-2}	4.8×10^{-2}	3.8×10^{-2}	2.5×10^{-3}	304
Mn	6.4×10^{-3}	2.3×10^{-2}	2.7×10^{-2}	3.4×10^{-3}	266
-	3.2×10^{-3}	1.5×10^{-2}	1.1×10^{-2}	3.8×10^{-3}	342
-	1.3×10^{-2}	4.5×10^{-2}	3.2×10^{-2}	3.1×10^{-3}	316
Co	6.4×10^{-3}	2.3×10^{-2}	1.2×10^{-2}	3.8×10^{-3}	362
-	3.2×10^{-3}	1.2×10^{-2}	6.1×10^{-3}	3.1×10^{-3}	355
-	1.3×10^{-2}	4.5×10^{-2}	2.9×10^{-2}	2.8×10^{-3}	383
Ni	6.4×10^{-3}	2.6×10^{-2}	1.2×10^{-2}	3.2×10^{-3}	357
-	3.2×10^{-3}	2.3×10^{-2}	8.8×10^{-3}	3.8×10^{-3}	358
-	1.3×10^{-2}	2.9×10^{-2}	2.9×10^{-2}	2.8×10^{-3}	247
Cu	6.4×10^{-3}	2.8×10^{-2}	2.0×10^{-2}	3.8×10^{-3}	-
-	3.2×10^{-3}	1.5×10^{-2}	1.2×10^{-2}	3.1×10^{-3}	291

a.BET surface area of silicalite = 295 m^2/g.

b.M = transition metal.

c.treated by calcination at 773k for 6h; exchanging with ammonium solution three times at room temperature and calcination at 773k for 6h again.

On the other hand, the metal to silicon ratios decreased after the ammonium exchange for the silicates of chromium, nickel, and cobalt. Most of all, only trace amount of chromium remained in the proton form samples of chromium silicate. Therefore, it can be concluded that most of chromium and part of cobalt and nickel in the metal silicates can be exchanged or washed out in the ammoniun sulfate solution.

Ion exchange capacity

Samples used to study their ion-exchange capacities were calcined manganese silicate (Mn/Si = 0.048), cobalt silicate (Co/Si = 0.045), nickel silicate (Ni/Si = 0.045), and copper silicate (Cu/Si = 0.029). The ammonia form of these metal silicates were prepared by treating the samples in 0.5M ammonium sulfate solution four times at 353K. They were then exchanged with 0.5M potassium sulfate solution four times at 353K. After washing with deionized water and drying at room temperature, these samples were analyzed by A.A. for transition metal and potassium content. The results were Mn/Si = 0.030 and K/Mn = 0.34 in manganese silicate; Co/Si = 0.015 and K/Co = 0.28 in cobalt silicate; Ni/Si = 0.013 and K/Ni = 0.32 in nickel silicate; Cu/Si = 0.023 and K/Cu = 0.15 in copper silicate. Any transition metals which are located in the framework of the metal silicate might provide sites for ion exchange. Since all the K/M values were less than 0.5, the potassium exchange experiments demonstrate that only samll portion of the manganese, cobalt, nickel, and copper can be incorporated in the framework of calcined metal silicates. In other words, most of transition metals within the calcined metal silicate are on the defect sites of the frame work.

Thermal analysis under air

Figure 2 shows the TGA and DTA profiles of silicalite and manganese silicate (Mn/Si = 0.023). Before 423K, the weight loss accompanied with an endothermic band (detected by DTA) was from the desorption of physically

adsorbed water. Between 423 and 533K, and between 533 and 603K, the weight loss accompanied with endothermic phenomena were from the desorption of chemisorbed water and physically adsorbed TPA (tetrapropylammonium compounds), respectively. Between 603 and 823K, the significant weight loss with an exothermic phenomenum was due to TPA combustion[17]. In addition, around 1200K, small exothermic bands were found on DTA; nevertheless, there were no apparent weight losses observed. This is consistent with a change of crystal phase. All the other metal silicates synthesized in this research generated similar TGA and DTA profiles.

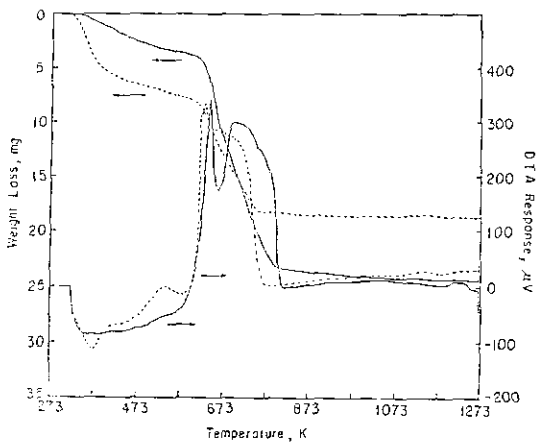

Fig. 2. TGA and DTA profiles of silicalite and manganese silicate (Mn/Si = 0.023); silicalite (—); manganese silicate (-----).

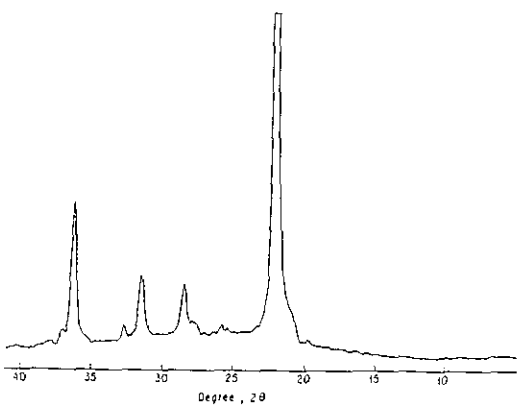

Fig. 3. The common XRD pattern of metal silicate and silicalite after heating to 1273 K.

The phase changes around 1200K were confirmed by examining the XRD patterns of silicalite and the metal silicates before and after heat treatment at these temperatures under air. Although the samples retained their highly crystalline ZSM-5 pattern at 1073K, Figure 3 shows the typical ZSM-5 structure collapse and change to dense phases after heating to 1273K. Therefore, we define the temperature around 1200K, at which a DTA exothermic phenomenum occurs, as the degradation temperature. Table 2 lists the degradation temperature of each sample as a function of metal to silicon ratio. It is found that the degradation temperature decreased generally with the increase of metal loading for each metal silicate series. These results suggest that the thermal stability of a given metal silicate decreases with an increase in metal loading.

The amount of physisorbed water, chemisorbed water and TPA measured from TGA experiments are also tabulated in Table 2. The amount of physisorbed water was found to increase with an increase in metal loading, with silicalite having the least amount of physisorbed water. These results suggest that the addition of transition metal

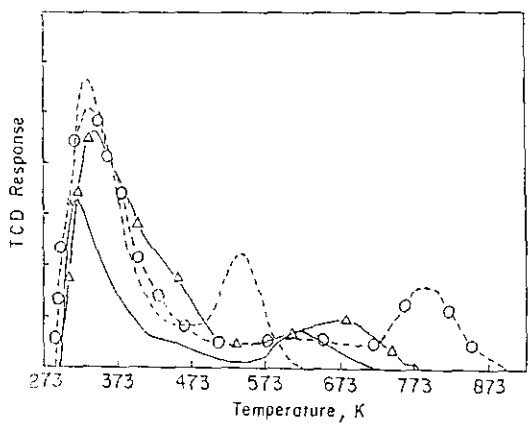

Fig. 4. TPD profiles of ammonia over HZSM-5, silicalite and copper silicate. Peak intensity of HZSM-5 is reduced to half of the original. HZSM-5, Al/Si = 0.017 (-Δ-Δ-); silicalite (-O-O-); Cu/Si = 0.020 (----); Cu/Si = 0.029 (—).

Table 2. Degradation Temperature and Desorption Amount from Silicate with ZSM-5 Structure

	M/Si after ammonium treatment	degradation temperature, K	Weight of physical desorption Water, g/g of catalyst	Weight of chemisorption Water and TPA, g/g of catalyst
chromium silicate	$8.4 * 10^{-4}$	1128	$76 * 10^{-3}$	0.14
	$6.1 * 10^{-4}$	1208	$38 * 10^{-3}$	0.15
	$4.1 * 10^{-5}$	1258	$27 * 10^{-3}$	0.15
manganese silicate	3.8×10^{-2}	1153	$307 * 10^{-3}$	0.14
	$2.7 * 10^{-2}$	1158	$70 * 10^{-3}$	0.16
	$1.1 * 10^{-2}$	1218	$26 * 10^{-3}$	0.15
cobalt silicate	$3.2 * 10^{-2}$	1223	$24 * 10^{-3}$	0.15
	$1.2 * 10^{-2}$	1243	$16 * 10^{-3}$	0.15
	$0.61 * 10^{-2}$	1218	$22 * 10^{-3}$	0.15
nickel silicate	$2.9 * 10^{-2}$	1243	$41 * 10^{-3}$	0.15
	$1.2 * 10^{-2}$	1243	$31 * 10^{-3}$	0.15
copper silicate	$2.9 * 10^{-2}$	1163	$63 * 10^{-3}$	0.16
	$1.2 * 10^{-2}$	1168	$32 * 10^{-3}$	0.17
Silicalite	0	1223	$10 * 10^{-3}$	0.15

(either Cr, Mn, Co, Ni, or Cu) in silicalite or metal silicates can increase their hydrophilic behavior. Furthermore, it was found that the amount of chemisorbed water is much less than the amount of TPA in each sample (Table 2) and that the TPA retained in the intracrystalline channels can act either as TPA^+ on anion sites in the framework or as templates for crystallization[17-19]. Thus, the approximately equivalent amount of TPA found in most of the metal silicates and silicalite may suggest the same intracrystalline channel formation in these catalysts during the crystallization process.

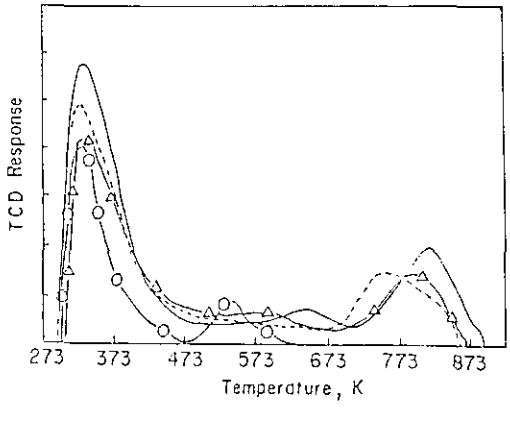

Fig. 5. TPD profiles of ammonia over manganese silicate and nickel silicate. Mn/Si = 0.038 (-O-O-);Mn/Si = 0.011 (-Δ-Δ-);Ni/Si = 0.029 (——); Ni/Si = 0.012

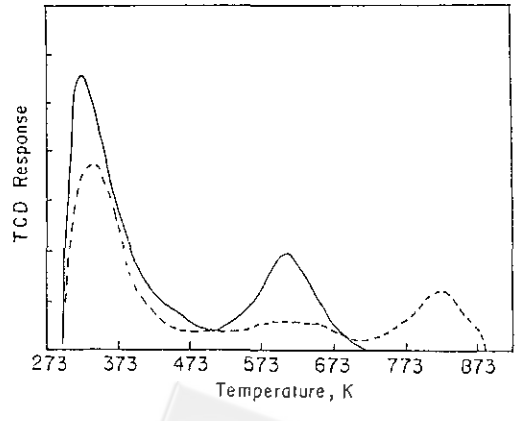

Fig. 6. TPD profiles of ammonia over cobalt silicate. Co/Si = 0.032 (——) ; Co/Si = 0.006 (-----).

Table 3. Product Distribution of Ethanol Conversion over Metal Silicate with ZSM-5 Structure

metal, M	Al	Al	Al	Al	Cr	Cr	Cr	Mn	Mn	Mn
M/Si	2.0×10^{-3}	3.6×10^{-3}	1.1×10^{-2}	1.7×10^{-2}	4.1×10^{-5}	6.1×10^{-4}	8.4×10^{-4}	0.11×10^{-2}	1.1×10^{-2}	3.8×10^{-2}
conversion	1.0	1.0	1.0	1.0	1.0	0.99	0.38	1.0	1.0	0.39
selectivity, %										
diethylether	0	0	0	0	0	0	92.5	0	0	0
C_1	0	0	0.01	0.05	0	0	0	0.02	0	0
C_2	88.6	55.4	7.3	2.3	68.9	96.4	5.7	32.6	93.4	10.5
C_3	3.2	8.9	12.6	14.1	7.1	1.2	1.5	11.3	2.0	4.1
C_4	3.8	14.3	24.5	25.5	10.7	1.1	0.2	19.2	2.0	10.7
C_5	2.2	8.8	12.6	14.9	6.1	0.9	0	10.7	1.1	0
C_6	1.5	4.9	6.6	6.0	3.7	0.3	0.03	6.4	0.02	0
C_7	0.5	2.6	5.4	4.3	1.9	0	0	5.3	0.3	0
C_8+	0.2	2.4	8.7	4.5	0.7	0	0	4.8	0.1	0
aromatics	0.05	2.6	22.3	28.3	1.1	0	0	9.5	0	0
acetaldehyde	0	0	0	0	0	0	0	0	0	64.2
metal, M	Co	Co	Co	Co	Ni	Ni	Ni	Cu	Cu	Cu
M/Si	0.3×10^{-2}	6.1×10^{-3}	1.2×10^{-2}	3.2×10^{-2}	0.9×10^{-2}	1.2×10^{-2}	2.9×10^{-2}	0.1×10^{-2}	1.2×10^{-2}	2.9×10^{-2}
conversion	1.0	1.0	0.9	0.17	1.0	0.97	1.0	1.0	0.35	0.17
selectivity, %										
diethylether	0	0	10.6	26.5	0	0	0	0	55.6	6.5
C_1	0	0	0	0.4	0.14	0.24	0.43	0	0.01	0.04
C_2	82.6	91.7	83.6	9.3	45.2	66.7	30.0	82.6	14.5	1.1
C_3	4.4	2.6	2.1	6.9	9.4	6.0	11.8	4.9	3.4	0.5
C_4	5.6	2.7	1.9	12.0	16.3	14.5	18.5	5.8	3.5	0
C_5	3.4	1.4	0	0	10.4	4.4	11.6	3.5	0.2	0
C_6	2.1	1.1	0.4	0.7	6.1	3.9	7.3	2.2	0.4	2.6
C_7	1.1	0.4	0.1	0.3	4.2	1.4	5.8	0.8	0	0.7
C_8+	0.4	0.1	0	0	3.5	1.6	4.4	0.1	0	0.8
aromatics	0.4	0	0	0	4.8	1.2	10.1	0.1	0	0.04
acetaldehyde	0	0	1.3	43.8	0	0	0	0.01	22.5	84.6

TPD of ammonia

Figures 4, 5, and 6 show the TPD of ammonia on ZSM-5, silicalite, and metal silicates (except chromium silicate) of the proton form. Two different metal loadings were investigated in each metal silicate series. In the case of ammonia desorption on HZSM-5 and silicalite, three desorption bands around 353K, 463K, and 673K from HZSM-5, and two desorption bands around 353K and 773K from silicalite can be observed in Figure 4. The bands around 353K and 463K were from physically and weakly chemically adsorbed ammonia, the band around 673K was from ammonia adsorbed on the zeolite hydroxyl group, and the band around 773K was from the dehydroxylation and the desorption of ammonia from the strong Bronsted acid sites or the Lewis acid sites[20].

In the cases of ammonia desorption on metal silicates, ammonia desorption bands between 473 and 673K, which may be associated with ammonia adsorbed on hydroxyl groups in zeolite, can be observed in Figures 4, 5, and 6. Similar desorption bands from gallium silicate and ferrisili-

Table 4. Catalytic Properties Characterized by Ethanol Conversion

Catalytic property	Calculation formula
dehydration	conversion x C_2^+ selectivity
dehydrogenation	conversion x acetone selectivity
oligomerization	(C_3^+ + aromatics) selectivity /(C_2^+ + aromatics) selectivity
cracking	(C_3 + C_5 + C_7) selectivity /(C_3^+ + aromatics) selectivity
aromatics	aromatics selectivity /(C_6^+ + aromatics) selectivity

cate in this temperature range have been reported[21]. These band intensities increased with the increase of metal loading in manganese, cobalt, and nickel silicates. On the other hand, the band intensities decreased and desorption teaperature incrcased with copper loading in copper silicate, which may be due to copper oxides formation in zeolite. The formation of copper oxides might decrease the amount of acidic sites for the ammonia adsorption. Note that in this desorption temperature range, nickel silicate had the maximun desorption temperature at 643K, which was higher than 603K of cobalt silicate, 613K of copper silicate, and 533K of manganese silicate.

The desorption bands between 773K and 823K from dehydroxylation or strong acidic sites of metal silicate were observed with some of the samples shown in Figures 4, 5, and 6. However, the higher metal loaded samples of manganese and cobalt silicate, and both copper silicate samples had no bands within this temperature range. This may be because their strong acidic sites or dehydroxylation sites were occupied by metal hydroxide or metal oxides. Note again, nickel silicate was the only higher metal loading

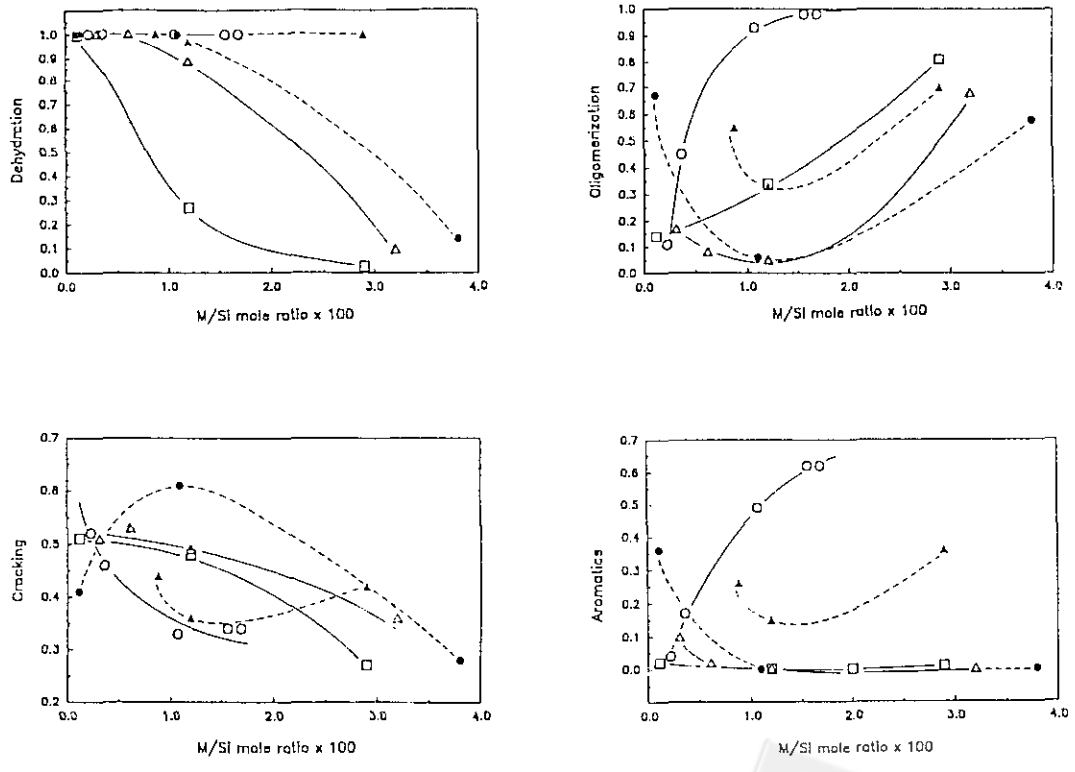

Fig. 7. Effect of metal to silicon ratios on catalytic behaviors characterized by ethanol conversion. HZSM-5 (-O-O-); manganese silicate (- - •- - •- -); cobalt silicate (-Δ-Δ-); nickel silicate (-▲-▲-); copper silicate (-□- □).

silicate which had a desorption band in this temperature range. Therefore, TPD of ammonia suggests that nickel silicate has stronger acid sites than the other transition metal silicates studied in this research.

Ethanol conversion

Ethanol conversion was carried out over metal silicates of proton form and HZSM-5. These catalysts maintained stable activity during six hours running, except for the copper silicates and cobalt silicate with Co/Si = 0.032. Table 3 lists the ethanol conversion and the product selectivity of each catalyst. The selectivity is defined as the weight of a specific product divided by the total weight of all the hydrocarbon products. The experimental data between the third and the fourth hour was used for the calculation. From the product distribution we can classify the following reaction sequence occuring in metal silicates and HZSM-5 : 1. dehydration of ethanol to produce diethylether and ethylene; 2. dehydrogenation of ethanol to produce acetaldehyde; 3. oligomerization of ethylene to form larger hydrocarbons; 4. cracking of oligomerized products to produce hydrocarbons with odd carbon numbers (larger than or equal to 3); 5. formation of the aromatics from the cyclization of C_6 or hydrocarbons larger than C_6 (cyclic hydrocarbons smaller than C_6 were not observed). Accordingly, each catalytic property is defined in Table 4. Through the product distribution data of ethanol conversion, we can characterize quantitatively the catalytic properties of dehydration, dehydrogenation, oligomerization, cracking, and formation of the aromatics

Figures 7 shows the quantitative results of catalytic properties as a function of metal to silicon ratio. Chromium silicates are excluded from these analyses because the metal to silicon ratios are too low. Also, dehydrogenation activity is not included in Figure 7, however it is shown by the selectivity of acetaldehyde in Table 3. While Table 3 indicates no dehydrogenation activity for HZSM-5 and nickel silicate, dehydrogenation activity is shown for manganese, cobalt, and copper silicates. This activity increases with an increase in metal loading.

Consistent with its high acidity as demonstrated from the previous ammonia desorption studies, nickel silicate is the only "highly" loaded metal silicate which has compatible catalytic activities of dehydration, oligomerization, cracking, and formation of the aromatics as HZSM-5 (Figure 7). For the other metal silicates, the dehydration and the formation of the aromatics decrease with the increase of metal loading, which is in contrast to the persisting and the increasing activities of HZSM-5. However, when metal to silicon ratio is larger than 0.01 in metal silicates, similar dependence of cracking and oligomerization on metal loading as that of HZSM-5 can be observed in Figure 7. As a result, it can be found that the cracking property decreases and the oligomerization increases with the increase of metal loading. Moreover, with the same metal to silicon ratio, every transition metal silicate has higher cracking property than HZSM-5. The doping of transition metal within ZSM-5 crystals may increase the cracking property of the zeolite. Notably, metal silicates with low M/Si ratios show similar activities as HZSM-5 with low Al/Si ratios (Figure 7). The trace amount of aluminum in these metal silicates (Table 1) plays the important role in contributing the catalytic activity.

From the reaction sequence of ethanol conversion it is understood that the formation of hydrocarbons larger than ethylene through oligomerization follows the dehydration of ethanol to form ethylene. Since Figure 7 indicates the decreasing trend of dehydration and the increasing trend of oligomerization over metal silicates with M/Si larger than 0.01, we can conclude that the low selectivity of oligomerized products over metal silicates with high M/Si ratio, listed in Table 3, is due to their low dehydration activity rather than low oligomerization activity.

CONCLUSION

1. Chromium, manganese, cobalt, nickel, and copper can be prepared in metal silicate with ZSM-5 structure through hydrothermal method; nevertheless, most of chromium and part of cobalt and nickel in calcined metal

silicate can be exchanged or washed out in the ammonium sulfate solution.

2. The thermal stability decreases and the hydrophilic behavior increases with the increase of transition metal loading within metal silicate

3. Small portion of transition metal within metal silicate has ion exchange ability which may demonstrate the existence of transition metal within the framework.

4. The TPD of ammonia and the ethanol conversion reaction indicate that nickel silicate has the highest acidity among metal silicates studied in this research; moreover, only nickel silicate has compatible catalytic acidity to HZSM-5 for ethanol conversion.

5. Manganese, cobalt, nickel, and copper silicates have stronger catalytic property for cracking and weaker catalytic properties for dehydration, oligomerization, and cyclization to the aromatics than HZSM-5

6. HZSM-5 and nickel silicate have no dehydrogenation catalytic property; on the other hand, the dehydrogenation catalytic properties of manganese, cobalt, and copper silicates increase with the increase of metal loading

ACKNOWLEDGMENT

The authors wish to thank Mr. C-Y Tai for doing TGA and DTA measurement, and Mr. C. Lin for determining ion exchange capacity and doing A. A. analysis

Received July 29, 1989

Key Word Index-

transition metal; ZSM-5; ethanol conversion.

REFERENCES

1. Haag, W.O. ; Lago, R.M ; Weisz, P.B. *J. Chem. Soc Faraday Dis*. **1981**, *72*, 317.
2. Argauer, K J ; Landolt, G.R., U .S. Patent 3702886, **1972**.
3. Meisel, S. L.; McCullough, J. P.; Lechthaler, C. H.; Weisz, P. B. *Chem. Tech*. **1976**, 86.
4. Chang, C. D.; Silvestri, A. J. *J. Catal*. **1977**, *47*, 249.
5. Nastro, A.; Sand, L. B. *Zeolite*, **1983**, *3*, 57.
6. Gabelica, Z.; Derouane, E. G.; Blom, N. in ACS Symposium Series 248 on 'Catalytic Material: Relationship between Structure and Reactivity', 220, **1984**.
7. Ruthven, D. M., "Principles of Adsorption & Adsorption Processes." John Wiley & Sons, New York, **1984**.
8. Miyamoto, A.; Medhanavyn, D.; Inui, T., Proc. 9th Intern. Cong.Catal., Canada, Vol. 1, P. 437, **1988**.
9. Szostak, R.; Nair, V.; Thomas, T. L. *J. Chem. Soc. Faraday Trans. I*, **1987**, *83*, 487.
10. Kotasthane, A. N.; Shiralkar, V. P.; Hegde, S. G.; Kulkarni, S. B. *Zeolite*, **1986**, *6*, 253.
11. Borade, R. B. *Zeolite*, **1987**, *7*, 398.
12. Inui, T.; Matsuda, H.; Yamase, O.; Nagata, H.; Fukuda, K.; Ukawa, T.; Miyamoto, A. *J. of Catal*. **1986**, *98*, 491.
13. Inui, T.; Medhanavyn, D.; Praserthdam, P.; Fukuda, K.; Ukawa, T.; Sakamoto, A.; Miyamoto, A. *Applied Catal*. **1985**, *18*, 311.
14. Jablonski, G. A.; Sand, L. B.; Gard, J. A. *Zeolite*, **1986**, *6*, 396.
15. McClune, W. F., "Powder Diffraction File", JCPDS, Pennsylvania, **1983**.
16. Lin, J-C.; Chao, K-J. *J. Chem. Soc. Faraday Trans. I*, **1986**, *82*, 2645.
17. Chao, K-J.; Chiou, R-H.; Cho, C-C.; Jeng, S-Y. *Zeolite*, **1984**, *4*, 2.
18. Kokotailo, G. T.; Lawton, S. L.; Olson, D. H.; Meier, W. M. *Nature*, **1978**, *272*, 437.
19. Swith, J. V.; Flanigen, E. M.; Bennett, J. M.; Grose, R. W.; Cohen, J. P.; Patton, R. L.; Kirchner, R. M. *Nature*, **1978**, *271*, 512.
20. Lok, B. M.; Marcus, B. K.; Angell, C. L. *Zeolite*, **1986**, *6*, 185.
21. Chu., C. T-W.; Chang, C. D. *J. Phys. Chem*. **1985**, *89*, 1569.